Advances in Water Resources 121 (2018) 1–8

Contents lists available at ScienceDirect

Advances in Water Resources

journal homepage: www.elsevier.com/locate/advwatres

Tidal asymmetry and residual sediment transport in a short tidal basin under sea level rise

Leicheng Guo[a,e,*], Matthew Brand[a], Brett F. Sanders[a,b], Efi Foufoula-Georgiou[a,c], Eric D. Stein[d]

[a] Department of Civil and Environmental Engineering, University of California Irvine, CA 92697, USA
[b] Department of Urban Planning and Public Policy, University of California Irvine, CA 92697, USA
[c] Department of Earth System Science, University of California Irvine, CA 92697, USA
[d] Southern California Coastal Water Research Project, Costa Mesa, CA 92626, USA
[e] State Key Lab of Estuarine and Coastal Research, East China Normal University, Shanghai 200062, China

ARTICLE INFO

Keywords:
Tidal basin
Tidal asymmetry
Sediment transport
Sea level rise
Morphodynamics

ABSTRACT

Tidal asymmetry in estuaries and lagoons (tidal basins) controls residual sediment transport, and quantifying tidal asymmetry is important for understanding the factors contributing to long-term morphological changes. Asymmetry in peak flood and ebb currents (Peak Current Asymmetry – PCA) controls residual transport of coarse sediment, and asymmetry in slack water duration preceding flood and ebb currents (Slack Water Asymmetry – SWA) controls residual transport of fine sediment. PCA and SWA are analyzed herein for Newport Bay, a tidal embayment in southern California, based on the skewness of tidal currents predicted for several stations by a hydrodynamic model. Use of skewness for tidal asymmetry is relatively new and offers several advantages over a traditional harmonic method including the ability to resolve variability over a wide range of time scales. Newport Bay is externally forced by mixed oceanic tides that are shown to be ebb dominant because of shorter falling tide than rising tide. Both PCA and SWA indicate ebb dominance that favors export of coarse and fine sediments, respectively, to the coastal ocean. However, we show that the ebb dominance of SWA is derived from the basin geometry and not the external forcing, while ebb dominance of PCA is linked to the external forcing and the basin geometry. We also show that tidal flats in Newport Bay play an important role in maintaining ebb dominated transport of both coarse and fine sediments. Loss of tidal flats could weaken PCA and reverse SWA to become flood dominant. Specifically, we show that sea level rise > 0.8 m that inundates tidal flats will begin to weaken ebb dominant PCA and SWA and that sea level rise > 1.0 m will reverse SWA to become flood dominant. This feedback mechanism is likely to be important for predicting long-term evolution of tidal basins under accelerating sea level rise.

1. Introduction

Tidal estuaries and lagoons around the world have been altered by human activities including coastal development, disruption of sediment supplies, and armoring of shorelines (UN, 2017). Impacts include loss of > 65% of sea grass and wetland habitat and depletion of > 90% of formerly important species (Lotze et al., 2006). In Southern California, for instance, over 48% of coastal wetlands have been lost since the middle 19th century, and the remaining systems are actively managed at a substantial cost for multiple objectives including flood defense, navigation, recreation, and water quality (Stein et al., 2014). Furthermore, accelerating rates of sea level rise are coming into focus as a major consideration for future planning. Globally averaged sea levels could rise 0.3–1.2 m by 2100 depending on emission scenarios (Kopp et al., 2014). As a result, tidal basins can anticipate a shift towards deeper water with less inter-tidal and upper marsh habitat particularly in developed coasts where inland migration of marshlands is constrained (Thorne et al., 2016, 2018). However, this trend may be offset through changes to sediment management practices including source control and enhanced marsh accretion. Doing so calls for an understanding of the natural processes at work especially the processes that control long-term morphological changes.

Residual transport of sediment from the cycling of flood and ebb tides serves as an important control on medium- to long-term morphological changes within tidal basins (Dronkers, 1986). Sediment transport rates generally scale with a third power of tidal currents, so small differences between flood and ebb currents can cause large differences in residual transport (Postma, 1961; Dronkers, 1986; de Swart and Zimmerman, 2009). The transport behavior of coarse (e.g., sand) and fine

* Corresponding author at: Department of Civil and Environmental Engineering, University of California Irvine, CA 92697, USA.
E-mail address: leicheng@uci.edu (L. Guo).

https://doi.org/10.1016/j.advwatres.2018.07.012
Received 12 January 2018; Received in revised form 28 June 2018; Accepted 19 July 2018
Available online 29 July 2018

(e.g., silt and clay) sediment is markedly different because the former is predominantly transported as bed load where the transport rate is a power function of current velocities with negligible time lag effects, while the latter is mixed throughout water column where it is predominantly transported as suspended load and strongly affected by time lag effects on initial motion and settling (Postma, 1954; Groen, 1967; van Rijn, 1993). Distinct indicators of residual sediment transport have been developed based on tidal asymmetry: differences between maximum tidal currents during flood and ebb (*peak current asymmetry*, PCA) serve as an indicator of residual flux of coarse sediment, and differences in slack water duration preceding flood and ebb (*slack water asymmetry*, SWA) serve to indicate residual flux of fine sediment (Dronkers, 1986). Similarly, net sediment transport in near shore is linked to asymmetry in currents from short waves (Ruessink et al., 2009; Chen et al., 2018). In practice, PCA and SWA are not easily computed because long records of tidal currents are not readily available, and thus an alternative indicator is *tidal duration asymmetry* (TDA) characterizing inequality between rising and falling tidal periods in tidal water levels. A water level record showing a shorter rising tide than falling tide will lead to stronger flood currents than ebb currents (flood asymmetry). Conversely, ebb dominance is featured by a shorter falling tide than rising tide that produces stronger ebb currents than flood currents. TDA is much more widely discussed because of availability of tidal water level data. However, TDA is not a substitute for PCA. Tidal currents are far more sensitive to basin geometry (e.g., channels, shoals and tide flats) and external forcing (e.g., river discharge) than surface water heights, thus PCA is still preferred in indicating residual sediment transport.

There have been numerous studies of tidal asymmetry based on time series of water level and currents with the goal of deepening understanding of residual sediment transport and long-term morphological change (Postma, 1961; Dronkers, 1986; de Swart and Zimmerman, 2009; Leonardi and Plater, 2017). Previous research indicates that tidal basins with limited tidal flats and insignificant river discharges are flood-dominated (Speer and Aubrey, 1985; Lanzoni and Seminara, 2002; Guo et al., 2016a). Inter-tidal flats tend to promote stronger ebb currents and may result in ebb dominance in short tidal basins (Fitzgerald and Nummedal, 1983; Friedrichs and Aubrey, 1988), and freshwater discharge intuitively strengthens ebb currents and elongates falling tides (Godin, 1985; Guo et al., 2014). Side channels developed for marinas and harbors can also impact tidal asymmetry (Alebregtse and de Swart, 2014; Roos and Schuttelaars, 2015; Stark et al., 2017). Oceanic tidal forcing is also an important consideration, as it can impart tidal asymmetry on tidal basins based on its astronomical constituents (Woodworth et al., 2005; Nidzieko, 2010; Jewell et al., 2012). In particular, mixed tidal regimes (an amplitude ratio $(A_{O1}+A_{K1})/(A_{S2}+A_{M2})$ in the range of 0.25–1.5) found along the West Coast of the U.S. are characterized by ebb dominance (Nidzieko, 2010). However, flood dominance within West Coast basins remains possible. For example, in the Tijuana River Estuary in California, an elevated sill at the mouth severely restricts ebb flows and thus promotes flood dominance (Nidzieko, 2010). Clearly, asymmetry in currents within tidal basins depends on numerous factors related to basin geometry and external tidal forcing. We can therefore expect that residual sediment transport processes regulating long-term morphological change will be sensitive to human interventions that alter basin geometry (e.g., dredging, development and habitat restoration) and sea level rise, which deepens basins. Moreover, site-specific assessment of residual sediment transport can help to inform coastal management activities such as channel dredging, sediment placement and wetland restoration.

In this study, we use a hydrodynamic model of an important tidal basin in southern California, Newport Bay, to simulate tidal currents and enable analysis of PCA and SWA. Following calibration of the model, the PCA and SWA are quantified and then additional scenarios are modeled to examine how PCA and SWA respond to: (a) changes to basin geometry (tidal flats and side channels) influenced by human activity, and (b) sea level rise. Tidal asymmetry is computed using a skewness method as recommended by Nidzieko (2010) for mixed tidal regimes. Traditional methods to quantify tidal asymmetry include harmonic indicators such as phase differences and amplitude ratios of the interacting tidal constituents, e.g., $2\theta_{M2}$-θ_{M4} and $\theta_{O1}+\theta_{K1}$-θ_{M2} (θ indicates the phase) (e.g., Speer and Aubrey, 1985; Friedrichs and Aubrey, 1988; van de Kreeke and Robaczewska, 1993; Hoitink et al., 2003). One advantage of the skewness method lies in its ability to cope with mixed tidal regime (see more discussions in Section 4.1). Variants of the skewness method have been developed to distinguish the contribution of different tidal interactions (Song et al., 2011), to explore fortnightly variations of tidal duration asymmetry (Guo et al., 2016b), and tidal current asymmetry (Gong et al., 2016). Combining a hydrodynamic model to simulate tidal currents with the skewness method to compute asymmetry offers a practical approach to anticipate the effects of proposed basin alterations and sea level rise on residual transport of coarse and fine sediment.

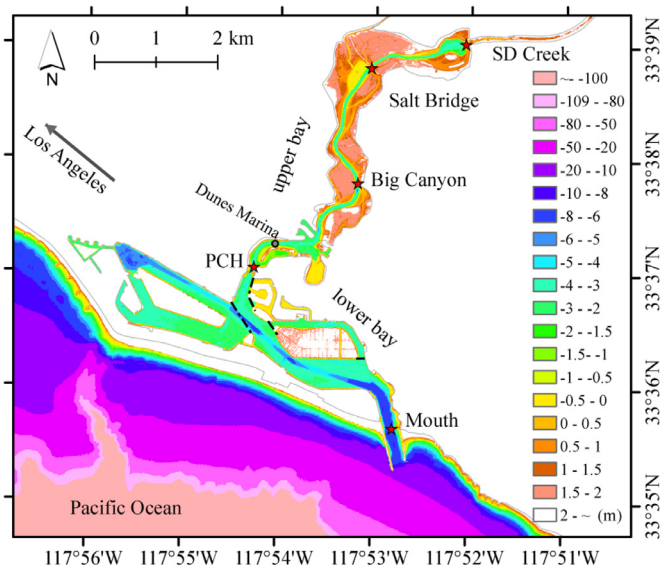

Fig. 1. Topography and bathymetry (color bar referenced to the mean lower low water which is ~0.8 m below the mean sea level) of Newport Bay in 2005. The black dot (Dunes Marina) indicate the site position with current measurement for model calibration and the red stars indicate the sites with model data output for tidal current asymmetry analysis. The dashed lines indicate artificial dikes used in the modeling scenarios that excludes side channels. (For interpretation of the references to color in this figure legend, the reader is referred to the web version of this article.)

This article is organized as follows. Section 2 will introduce the study area, the modeling setup and the skewness method used to quantify tidal asymmetry. Section 3 presents modeling results including impacts of basin geometry and sea level rise on tidal asymmetry. Discussion of the advantages and shortcomings of the skewness method and the implication of the model results are in section 4. Section 5 provides a brief summary of the findings in this work.

2. Method and materials

2.1. Site description

Newport Bay, located 60 km south of Los Angeles in California, is a short (~10 km), micro-tidal (mean tidal range of ~1.2 m) basin with broad inter-tidal flats in the upper bay (landward of Pacific Coast Highway (PCH)) and ample side channels in the lower bay (seaward of PCH) (Fig. 1). The upper bay is a wildlife refuge dominated by tidal marsh habitat, and its subtidal channels are periodically dredged as part of active sediment management programs to restore channel volume. The lower bay is a pleasure craft harbor with extensive shoreline development that is vulnerable to coastal flooding. Without major interventions, future sea level rise will result in chronic flooding of the developed ar-

eas of the lower bay (FloodRISE Project, 2017) and a transformation of upper bay to a system dominated by subtidal habitat (loss of inter-tidal marshes) (Thorne et al., 2016, 2018). Hence, there is interest in coordinating sediment management programs (e.g., reducing the frequency of dredging) with natural processes (i.e., tide- and/or river-induced residual sediment transport and consequent morphological changes) to cost-effectively adapt to higher sea levels while balancing multiple management objectives.

Because of its historical development, Newport Bay departs from the archetypal funnel geometry of tidal estuaries. The bay mouth is fixed by two jetties built in the 1930 s. The inter-tidal flats in the upper bay account for nearly 70% of the wet surface area at high tide. The side channels in the lower bay provide extra space for tidal prism. The subtidal channel depth averages ~5 m within Newport Bay, with limited changes along the basin axially because of dredging activities.

Newport Bay is externally forced by mixed tides, where the ratio of diurnal and semi-diurnal tidal amplitudes, $(A_{O1} + A_{K1})/(A_{M2} + A_{S2})$, is 0.76. The mean tidal range is about 1.2 m at the mouth. The M_2 is the most important astronomical constituent, followed by K_1, O_1, S_2, N_2, and P_1. The other constituents are of secondary importance given amplitudes less than 0.05 m. The overtide (e.g., M_4) and compound tides (e.g., MS_4 and MN_4) have insignificant amplitudes (< 0.01 m) in adjacent coastal waters (limited tidal deformation because of open coasts and narrow shelf) and inside Newport Bay (mainly due to small basin length), thus their impacts in causing tidal asymmetry are negligible.

Due to a small basin length, the tides in Newport Bay have a standing wave form with only small amplification (several cm in the far western and northern reaches). The phase changes of the astronomical constituents are small, e.g., the high water time lag is < 25 min at the northern head compared to the bay mouth. Hence, the rise and fall of water levels is fairly uniform throughout the basin.

Freshwater input from San Diego Creek is small (~1 m^3/s) in the dry season (late Spring through early Fall) leading to well-mixed and highly saline conditions, but episodic storms lasting hours to few days can occur from late Fall through early Spring and cause river discharge of 100–1000 m^3/s and pulses of sediment supply and partial stratification in the upper bay (Trimble, 2003).

2.2. Model setup

The Delft3D model (Lesser et al., 2004) is applied to produce time series of tidal currents for analysis of PCA and SWA in Newport Bay. The model domain encompasses all subtidal and inter-tidal topography/bathymetry and extends several km offshore of the mouth. The model uses a curvilinear grid with a variable resolution as fine as 5 m within the bay and up to 500 m offshore. Ground elevations are specified using a digital elevation model that combines sonar measurements of bathymetry with LiDAR measurements of subaerial topography (Gallien et al., 2011). Tidal dynamics are resolved using depth-integrated shallow-water equations that assume a hydrostatic pressure distribution, a uniform vertical distribution of horizontal velocity, and a constant fluid density. Tidal forcing of the model is achieved by specifying water level at the offshore boundary, and river forcing from San Diego Creek is achieved by specifying streamflow at the northern head of the basin. The model is calibrated against water levels and tidal currents measured during dry-weather periods by adjusting resistance parameters as described in the supplementary material (see Figs. S6 and S7 in the digital supplementary material).

Model scenarios considered in this study are defined by tidal and riverine forcing, and basin geometry. A baseline scenario representative of present-day dry-weather dynamics is configured assuming a small freshwater inflow (1 m^3/s) and mixed oceanic tides using six tidal constituents, M_2, S_2, N_2, O_1, K_1, and P_1 with amplitudes and phases taken from NOAA (https://co-ops.nos.noaa.gov, gauge: 9,410,660). Additional scenarios are considered to examine the role of basin geometry and sea level rise on tidal asymmetry. Scenarios to address the impacts of basin geometry are defined by excluding the inter-tidal flats in the upper bay (the tidal flats with an elevation above the mean low water are removed and only the subtidal channel remains) and excluding the side channels in the lower bay (impose thin dams at the connections of the side channels, see Fig. 1). The impacts of sea level rise are examined by scenarios considering sea level rise in the range of 0–1.5 m (15 scenarios with an increments of 0.1 m) on the present day morphology. Moreover, an additional simulation is run by imposing a symmetric sinusoidal M_2 component only at the seaward boundary. All model scenarios are run for a three-month period between May and August which captures perigean spring tides at the summer solstice.

2.3. Skewness approach

PCA and SWA are estimated using a skewness measure computed as follows:

$$\gamma(x) = \frac{\frac{1}{N-1}\sum_{i=1}^{N}\left(x_i - \bar{x}\right)^3}{\left[\frac{1}{N-1}\sum_{i=1}^{N}\left(x_i - \bar{x}\right)^2\right]^{3/2}} \quad (1)$$

where γ is skewness, x_i is the time series of sample signals, $\bar{x}$ is the mean value (expected value) of the samples, and N is the number of equal-distanced (hourly) time series data. Numerical models of tidal basins are generally configured to output time series of tidal water level η or tidal currents u which provides a basis for several alternative measures of tidal asymmetry (Table 1). In particular, PCA is estimated using Eq. (1) assuming $x = u$, SWA is computed assuming $x = du/dt$ which corresponds to velocity acceleration (Gong et al., 2016). In addition, TDA is also computed from time derivatives of tidal water levels, i.e., $x = d\eta/dt$ (see Table 1 and the supplementary material). The skewness method (Eq. (1)) has been widely used in earth sciences such as in detecting asymmetry in turbulence velocity fluctuations (Basu et al., 2007) and wave-generated currents (Ruessink et al., 2009), although with small modifications of the input signals for different purposes. One assumption of the skewness method is that the input signal is stationary which is satisfied in tide-dominated environments with insignificant or constant river discharges.

As indicated in Table 1, skewness calculations for PCA and SWA are made using a velocity threshold to minimize noise in results. The threshold is a lower limit for PCA and an upper limit for SWA, and it is not necessarily the same as the critical velocity for initial sediment motion. Preliminary analysis suggests that the absolute value of the skewness indicators of PCA and SWA will slightly increase and decrease, respectively, with an increasing velocity threshold in the range of 0.1–0.3 m/s, but not change sign. Using the same velocity threshold enables consistent comparison of the results between different scenarios. Furthermore, skewness is computed using a moving window (25 h) to capture subtidal variations (additional information is provided in the Supplementary Material).

3. Results

3.1. Baseline tidal currents and asymmetry

Tidal currents are maximum in the middle segment of Newport Bay between Big Canyon and PCH and exhibit strong spring-neap variations and daily inequality, as shown in Fig. 2 for a 24 h period in June under spring (Fig. 2A) and neap (Fig. 2B) conditions. The magnitude of peak ebb velocities tend to be larger than flood peak velocities at spring tides, and the opposite is true at neap tide (Fig. 2). Note that the changes in tidal heights across Newport Bay are relatively uniform because of short basin length.

PCA and SWA computed using a velocity threshold of 0.15 m/s (Fry and Aubrey, 1990) for the entire three-month record indicates ebb dominance throughout the system. Tidal asymmetry values for all scenarios are presented in Table 2. PCA indicates ebb-dominated transport of coarse sediment cross the basin with values of −0.36, −0.41, −0.30

Table 1
Indicators of tidal asymmetry (PCA, SWA, and TDA) computed by the skewness method.

Skewness measure	Description	Application	Function form	Data filtering
Peak Current Asymmetry (PCA)	unequal peak flood and ebb currents	residual coarse sediment transport	tidal currents, $\gamma_{PCA} = \gamma(u)$	use threshold $\|u\| > u_c$
Slack Water Asymmetry (SWA)	unequal high and low water slack duration	residual fine sediment transport	acceleration of tidal currents, $\gamma_{SWA} = \gamma(du/dt)$	use threshold $\|u\| < u_c$
Tidal Duration Asymmetry (TDA)	unequal rising and falling tidal duration	indicate PCA under quadrature phase relationship	time derivative of tidal height, $\gamma_{TDA} = \gamma(d\eta/dt)$	use time series of high water and low water

Table 2
Mean PCA and SWA based on skewness for all model scenarios at bay mouth, PCH, Big Canyon (BC) and Salt Bridge (SB).

		PCA				SWA			
No	Scenarios	Mouth	PCH	BC	SB	Mouth	PCH	BC	SB
N1	baseline	−0.36	−0.41	−0.30	−0.70	−0.29	−1.72	−1.79	−1.05
N2	M_2 tide only	−0.09	−0.08	−0.01	−0.08	−0.23	−1.41	−1.68	−0.76
N3	no tidal flats	−0.28	−0.20	−0.29	−0.71	0.32	0.64	0.95	0.84
N4	M_2 and no flats	−0.05	−0.01	−0.06	−0.05	0.31	0.68	0.71	0.78
N5	no side channel	−0.43	−−0.36	−0.33	−0.77	−0.70	−1.79	−1.86	−0.41
N6	no flat & channel	−0.36	−0.24	−0.29	−0.72	0.22	0.56	0.86	0.77
N7	SLR = 0.5 m	−−0.38	−0.32	−0.25	−0.56	−0.61	−2.00	−1.79	−0.62
N8	SLR = 1.0 m	−0.36	−0.27	−0.22	−0.53	−0.62	−1.76	−0.86	−0.13
N9	SLR = 1.5 m	−0.30	−0.21	−0.16	−0.50	0.00	0.02	1.67	1.11

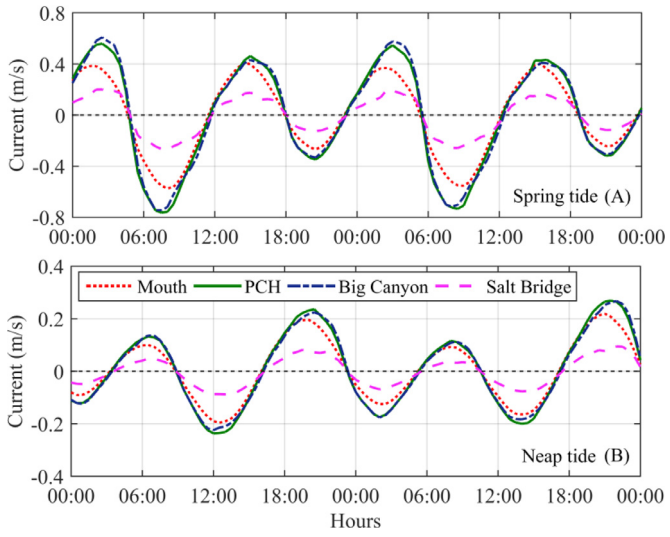

Fig. 2. Modeled time series of tidal currents at the bay mouth, PCH, Big Canyon and Salt Bridge of Newport Bay in the baseline scenario: (A) spring tide and (B) neap tide in June.

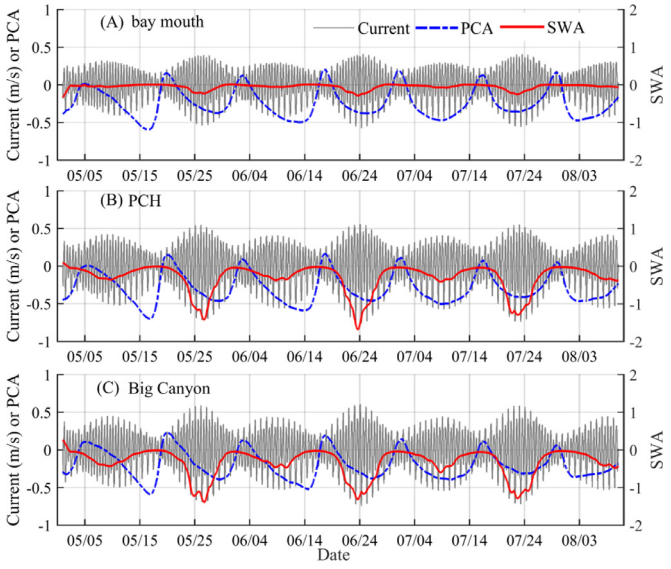

Fig. 3. PCA and SWA computed with a 25 h window at (A) bay mouth, (B) PCH, and (C) Big Canyon in the baseline scenario. Positive and negative currents correspond to flood and ebb, respectively.

and −0.70 at bay mouth, PCH, Big Canyon and Salt Bridge, respectively. It is consistent with negative skewness derived from tidal water level data which indicates overall shorter falling tide than rising tide (see the supplement). Similarly, SWA values of −0.29, −1.72, −1.79 and −1.05 at the bay mouth, PCH, Big Canyon and Salt Bridge, respectively, indicate ebb-dominated transport of fine sediment throughout the system. Spatially, SWA is the strongest in the middle segment of the bay between PCH and Big Canyon where tidal currents are highest.

Fig. 3 presents temporal variability in PCA and SWA at three stations for the three-month model simulation period based on a 25 h skewness calculation window. Both signals exhibit fortnightly variability but differ in shape and phase. PCA is similar across these stations with mostly negative values that typically reach a maximum absolute value sometime between spring and neap tides. Furthermore, positive values occur for a relatively short periods near the occurrence of neap tides when peak flood velocities are larger than peak ebb currents (Fig. 3). Negative peaks in SWA generally occur with the largest spring tide, and positive SWA are rare. Fig. 3 also shows that spatially, the SWA values are clearly greater (in magnitude) in the middle reaches of Newport Bay than at the mouth. Note that the subtidal SWA and PCA are not in phase.

The preceding analysis is repeated with external forcing by a (symmetric) M_2 tide. This produces nearly equal peak ebb and flood velocities, and it results in relatively small and negligible PCA compared to the baseline scenario, but measurable SWA that is comparable to the baseline scenario (Table 2 and Fig. S8). It suggests that tidal asymmetry embedded in the external mixed tides is the main control on PCA inside the basin, whereas SWA is internally generated inside the basin.

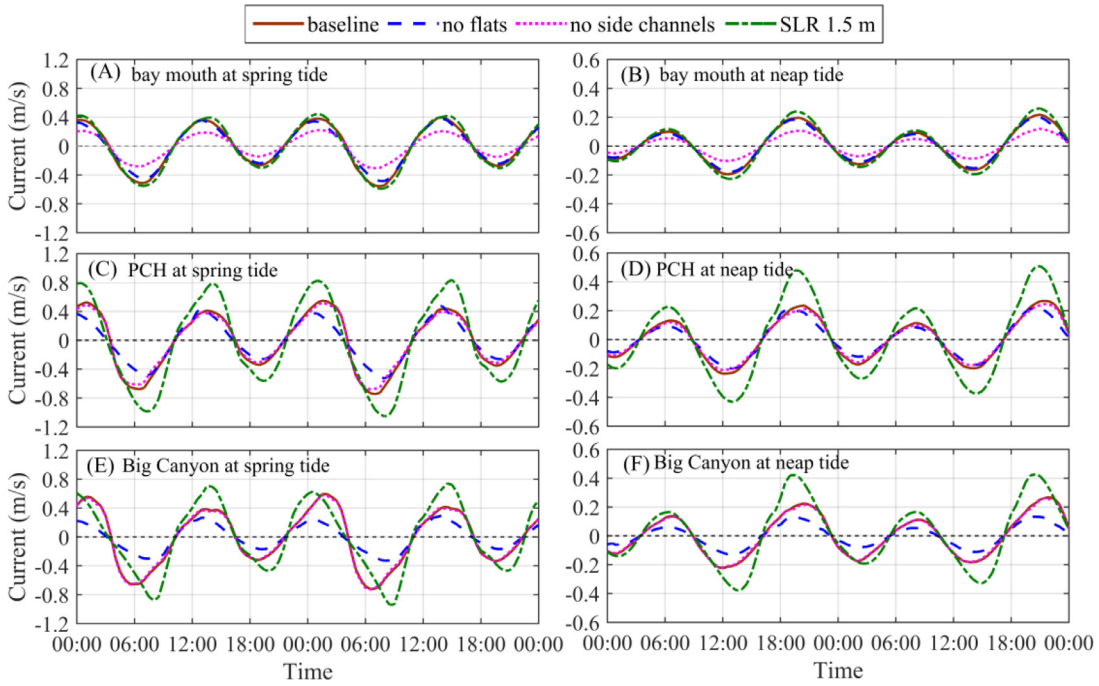

Fig. 4. Time series of modeled current velocities at the mouth (A, B), PCH (C, D), and Big Canyon (E, F) for different scenarios at spring tide (A, C, E) and neap tide (B, D, F). Positive is flood and negative is ebb.

3.2. Impact of basin geometry

Model scenarios reveal the impacts of side channels and tidal flats on tidal current magnitude and on PCA and SWA. Fig. 4 shows that excluding the inter-tidal flats in the upper bay results in slightly smaller currents, and the ebb currents decrease at a larger rate than flood currents especially in the upper bay as shown at Big Canyon and PCH. It is because the inter-tidal storage volume and tidal prism decrease in the absence of tidal flats thus tidal currents decrease. Moreover Fig. 4 also shows that excluding the side channels in the lower bay will reduce current magnitude at bay mouth. Specifically, tidal currents at the mouth are reduced by about 50% compared to the baseline scenario whereas the changes at PCH and Big Canyon are negligible. It is because the tidal prism at the bay mouth is significantly reduced by excluding the side channels because a smaller surface area and volume has to be drained.

Excluding tidal flats and side channels will increase the ebb dominance at spring tides and increase the flood dominance at neap tides, particularly at the bay mouth (see Fig. S9 in the supplement). The net PCA for 3-month data under scenarios representing major perturbations of system geometry shows that the system will remain ebb dominant with respect to residual coarse sediment transport, since PCA remains negative under all scenarios as shown in Fig, 5 and Table 2. However, the ebb dominance is weakened in the lower bay (PCH to mouth) from loss of tidal flats, which points to the potential for increasing accumulation of coarse sediment in lower bay.

Calculation of SWA (Table 2 and Fig. 5) shows that major changes in system geometry have the potential to reverse the residual transport of fine sediment. In particular, Fig. 5 shows that SWA is positive (flood dominance) without tidal flats and increases with distance from the mouth to Big Canyon; it subsequently decreases with further distance towards the head of the system. These changes suggest that loss of tidal flats in the upper bay will enhance accumulation of fine sediment therein, especially north of Big Canyon, which will potentially stimulate formation of tidal flats as a negative feedback. SWA would remain negative (ebb dominance) with the loss of side channels in the lower bay, and this condition would continue to favor export of fine sediment to the coastal ocean.

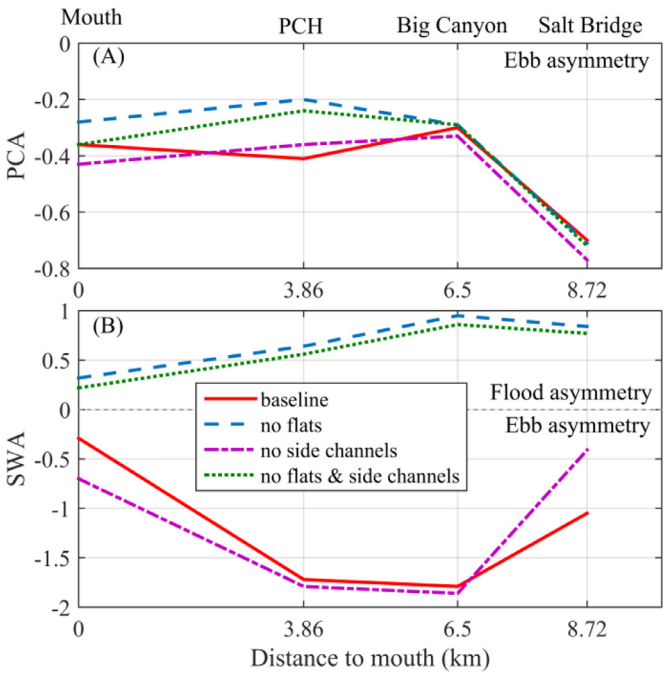

Fig. 5. Variations of (A) PCA and (B) SWA along Newport Bay for different scenarios considering basin configuration changes.

Tidal current strength reduces remarkably as well as current asymmetry in the scenario (N4) excluding tidal flats and forced by an M_2 tide only compared to the scenario (N2) including tidal flats (see Fig. S8 in the supplement). PCA in scenario N4 is small as that in the scenario (N2) forced by M_2 tide and with tidal flats while its SWA is similar to that in the scenario (N3) forced by six tidal constituents but without tidal flats (Table 2). These sensitivity model results show that the inter-tidal flats exert a primary control on SWA.

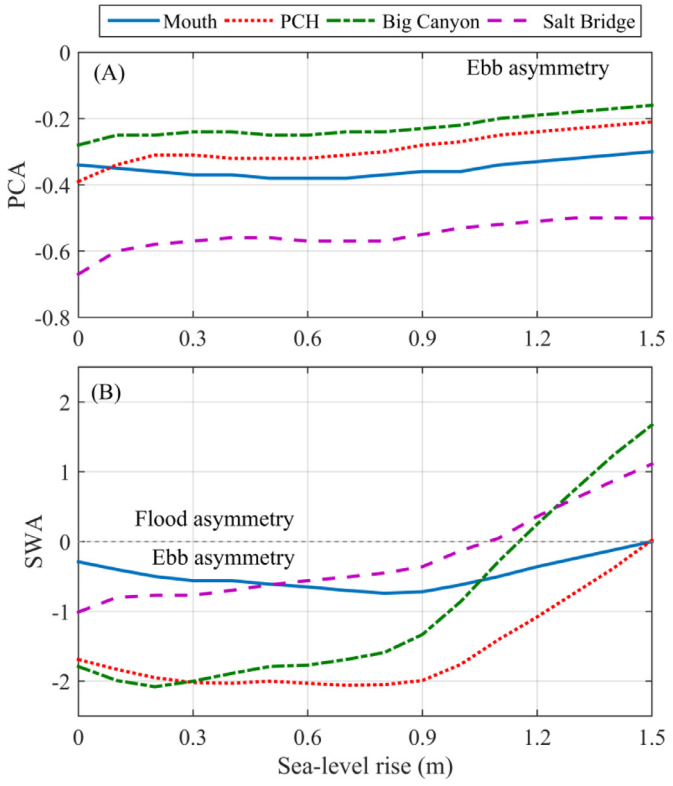

Fig. 6. Variations of (A) PCA and (B) SWA at bay mouth, PCH, Big Canyon and Salt Bridge with increasing magnitude of sea level rise on the present morphology.

3.3. Impact of sea level rise on PCA and SWA

Tidal surface amplitude changes are negligible with sea level rise < 1.5 m because of a short basin length and synchronous tides, whereas both ebb and flood currents increase from a proportional increase in tidal prism relative to channel cross-sectional area. Fig. 4 shows that the sensitivity of currents to 1.5 m of sea level rise is larger in the upper bay (PCH and Big Canyon) than the mouth. This effect is due to sea level rise causing a more significant increase of tidal prism owing to the presence extensive inter-tidal flats in the upper bay than the increase of cross-sectional area at PCH and Big Canyon due to confined section profile (see Fig. S10 in the supplement). Therefore current velocities increase under sea level rise compared to the baseline scenario.

Fig. 6 shows the impacts of 0–1.5 m of sea level rise on PCA and SWA, and the response is nonlinear. Sea level rise by 1.5 m reduces PCA and its impacts tend to be much stronger at spring tides in the upper bay (see Fig. S9). At the bay mouth, PCA is slightly enlarged by sea level rise < 0.6 m and but it is weakened with larger sea level rise (Fig. 6A). Inside the bay, ebb PCA is non-uniformly weakened with increasing sea level rise up to 1.5 m. Regarding SWA, Fig. 6B shows that sea level rise < 0.8 m results in increasing ebb dominance in the lower bay (PCH to bay mouth) but decreasing ebb asymmetry in the upper bay (Big Canyon to Salt Bridge). More importantly, a major change in SWA is predicted for sea level rise > 0.8 m: SWA nearly vanishes in the lower bay and switches to flood asymmetry in the upper bay under a high sea level rise, i.e., low water slack becomes shorter than high water slack (Table 2 and Fig. 6B). This results from low water slack periods becoming shorter than high water slack periods. These variations suggest that SWA is more sensitive to sea level rise than PCA and the upper bay is more sensitive to sea level rise more than the lower bay. It is because the mean sea level will change the water depth over tidal flats in the upper bay thus altering the slack water asymmetry.

The inflection point of 0.6–0.8 m corresponds to a change in the hypsometry of upper bay, whereby topography is relatively flat at lower elevations and relatively steep at higher elevations. Hence, the transition to flood dominance occurs as tidal flats are inundated by high sea levels and surface area increases with increasing water level at a slower rate (see Fig. S11 in the supplement).

4. Discussion

4.1. Advantage and shortcoming of the skewness method

We see that tidal asymmetry in Newport Bay exhibits strong subtidal variability with respect to its nature and magnitude (see Figs. 3 and S6). Similar subtidal variations of tidal asymmetry are also reported in previous studies. For instance, fortnightly variations of tidal asymmetry occur in both diurnal and mixed tidal regimes (Ranasinghe and Pattiaratchi, 2000; Guo et al., 2016b; Gong et al., 2016). Stronger tidal asymmetry is generally expected at spring tide compared to neap tides Wang et al., 1999). These facts indicate that strong subtidal variations of tidal asymmetry are not unique in Newport Bay but can be a universal phenomenon. The skewness method can be also used to quantify the contribution of different tidal interactions, e.g., M_2–O_1–K_1 and S_2–K_1–P_1, when combined with tidal harmonic data (Song et al., 2011). Overall the skewness method has several strengths in characterizing tidal asymmetry regarding: ((1) its ability to resolve subtidal variations of tidal asymmetry and (2) its ability to measure the net effects of multiple tidal interactions which possibly augment or reduce each other in creating net tidal asymmetry. The harmonic method is also able to reveal fortnightly variations of tidal asymmetry when considering the modulation effect of S_2 (Wang et al., 1999). The shortcoming of the skewness proxy lies in its lack of a strong physical background. The skewness method provides a complementary option for tidal asymmetry characterization in mixed tidal regime except the harmonic method.

4.2. Controls on tidal asymmetry in newport bay

The sensitivity simulations results confirm that the oceanic tides control the ebb dominance of PCA inside Newport Bay. The oceanic tides off the Southern Californian coasts are characterized by ebb dominance of TDA (Nidzieko, 2010). In tidal surface waves, it is featured by higher high water preceding lower low water (see Figure S6), leading to stronger ebb currents than flood currents and consequent ebb PCA. In harmonic, the ebb dominance is mainly controlled by the M_2–O_1–K_1 triad interactions with a phase difference of $\theta_{O1} + \theta_{K1} - \theta_{M2}$ in the range of 180–360°. Such phase differences may vary spatially in long basins such as San Francisco Bay and Chesapeake Bay where loss of inter-tidal flats to reclamation and sea level rise have modification effects on tidal wave propagation and deformation (Godin and Martinez, 1994; Holleman and Stacey, 2014; Lee et al., 2017). In short basins such as Newport Bay, however, changes to basin topography have limited effects on tidal wave propagation except for prominent features such as sills at the outlet capable of restricting tide propagation (Nidzieko, 2010).

Inter-tidal flats are the secondary factor in inducing slightly stronger ebb currents and ebb PCA. The impacts of inter-tidal flats on PCA are much more apparent at PCH because of the presence of broad inter-tidal flats inland of PCH. The tidal amplitude to water depth ratio in Newport Bay is 0.12 and the mean ratio of inter-tidal flat storage volume to channel volume is ~1.0 in the upper bay and ~0.3 for Newport Bay as a whole, suggesting a hypsometry favoring ebb dominance according to Friedrichs and Aubrey (1988). Moreover, we find that the inter-tidal flats are the prime control of ebb SWA in Newport Bay.

Sea level rise can have significant impacts on tidal asymmetry because mean water depth increases with sea level rise while tidal wave amplitude changes little, thus the tidal amplitude to water depth ratio decreases as well as the ratio of inter-tidal flat storage volume to channel volume. This effect is similar to that of decreasing tidal flat

storage which decreases ebb dominance (Friedrichs and Aubrey, 1988; Fortunato and Oliveira, 2005). The tidal flats in the upper bay have an elevation in the range of 0.5–1.5 m and the upper bay is surrounded by steep bluffs. Therefore, high sea level rise will convert nearly all the inter-tidal flats into subtidal flats (see Fig. S11 in the supplement), thus substantially eliminating inter-tidal flat storage volume and its impacts on SWA. This feedback can explain the SWA switch from ebb to flood by high sea level rise (see Table 2 and Fig. 6).

4.3. Implications on residual sediment transports

The ebb dominance of both PCA and SWA in the present-day Newport Bay favors seaward export of both coarse and fine sediments. This is beneficial for maintaining channel depth for navigation and channel volume for reducing flood risk, but it is to the disadvantage of tidal flat accretion and salt marsh conservation under rising sea levels. Sea level rise points to an overall decrease of ebb PCA and SWA inside the bay, suggesting that seaward sediment export will become smaller the higher sea level rises. This represents a potentially important feedback mechanism that could reduce tidal flats and salt marsh loss in response to sea level rise.

Another significant factor controlling tidal flats accretion in Newport Bay is deposition of river-supplied sediment. Sediment is supplied to the system mainly by episodic storm flows that occur primarily in winter and spring. It leaves deposits in upper bay which are later transported seaward by tides. The relatively weak but persisting flushing by tides likely explains the historical infilling of the upper bay and tidal flat formation therein. Moreover, these dynamics suggest that long-term morphological change in Newport Bay is characterized by episodic filling from storm events, human intervention (e.g., dredging and regarding for marsh restoration) and long-term redistribution by tidal currents. Models that couple natural hydro-morphodynamic and biological processes (e.g., Kirwan and Murray, 2007) with human processes (Di Baldassarre et al., 2015) and sea level rise are needed to improve future predictions of coastal changes in Newport Bay and other coastal basins.

Several other factors besides PCA and SWA measured along the main basin axis contribute to residual sediment transport and subsequent morphodynamic changes in tidal basins. For example, residual circulations between meandering channels and tidal flats can induce suspended sediment transport toward flats in the presence of settling and scour lag effects (de Swart and Zimmerman, 2009). Both temporal spatial lag (Groen, 1967) and spatial settling lag effects (Postma, 1954) can cause significant net transport of fine sediments toward tidal flats. Gravitational circulation generated by interactions between freshwater and intruded salt water will trap sediment in the lower bay by reducing seaward sediment flushing. Tidal asymmetry differs from these processes of local importance because its impacts on residual sediment transport are evaluated at large space and long time scales.

5. Conclusions

Tidal asymmetry can be expressed in several ways useful for analysis of residual transport of coarse and fine sediments, and here two measures of tidal asymmetry, i.e., PCA and SWA, based on a statistical skewness method are developed to better understand how basin geometry and sea level rise change tidal asymmetry.

Model result shows that Newport Bay is overall ebb dominant regarding both PCA and SWA, with stronger peak ebb velocities than peak flood and shorter high water slack than low water slack. A moving window analysis also reveals stronger ebb dominance at spring tides than neap tides.

Sensitivity scenarios suggest that the oceanic tides are the major contributor of ebb-dominated PCA and inter-tidal flats are a major contributor to ebb-dominated SWA. In the absence of tidal flats, ebb dominant transport of coarse sediment is weakened in the lower bay and ebb dominant transport of fine sediment is reversed throughout the bay to become flood dominant. The side channels in the lower bay enlarge tidal currents at the mouth and increase both PCA and SWA. Small changes in sea levels can slightly increase PCA and SWA at the bay mouth while high sea level rise will cause overall decrease of PCA and SWA throughout the basin, and eventually a switch from ebb to flood SWA in the upper bay.

These findings imply net seaward transport of both coarse and fine sediments in Newport Bay. The fact that Newport Bay's capacity to export sediment is reduced with increasing sea level rise points to a potentially important feedback mechanism to slow or possibly stop the transformation of inter-tidal wetland habitat to subtidal wetland habitat which has been predicted for numerous tidal basins in California by 2100 (Thorne et al., 2016, 2018). This highlights the need for coupling of hydrodynamic, morphodynamic and biological processes to better characterize long-term coastal changes.

Acknowledgements

This work is financially funded by NOAA project "Codevelopment of modeling tools to manage sediment for sustainable and resilient coastal lowland habitat in Southern California". L. Guo is also partly supported by National Natural Science Foundation of China (Nos. 41506105; 51320105005, 51739005).

Supplementary materials

Supplementary material associated with this article can be found, in the online version, at doi:10.1016/j.advwatres.2018.07.012.

References

Alebregtse, N.C., de Swart, H.E., 2014. Effect of a secondary channel on the non-linear tidal dynamics in a semi-enclosed channel: a simple model. Ocean Dyn. 64, 573–585.
Basu, S., Foufoula-Georgiou, E., Lashermes, B., Arneodo, A., 2007. Estimating intermittency exponent in neutrally stratified atmospheric surface layer flows: a robust framework based on magnitude cumulant and surrogate analysis. Phys. Fluid 19, 115102. https://doi.org/10.1063/1.2786001.
Chen, X., Li, Y., Chen, G.F., Wang, F.J., Tang, X.L., 2018. Generation of net sediment transport by velocity skewness in oscillatory sheet flow. Adv. Water Resour. 111, 395–405.
de Swart, H.E., Zimmerman, J.T.F., 2009. Morphodynamics of tidal inlet systems. Ann. Rev. Fluid Mech. 41, 203–229.
Di Baldassarre, G., Viglione, A., Carr, G., Kuil, L., Yan, K., Brandimarte, L., Blöschl, G., 2015. Perspectives on socio-hydrology: capturing feedbacks between physical and social processes. Water Resour. Res. 51, 4770–4781.
Dronkers, J., 1986. Tidal asymmetry and estuarine morphology. Neth. J. Sea Res. 20 (2/3), 107–131.
Fitzgerald, D.M., Nummedal, D., 1983. Response characteristics of an ebb-dominated tidal inlet channel. J. Sediment. Petrol. 53 (3), 838–845.
FloodRISE Project, 2017. Online Flood Hazard Viewer. University of California, Irvine Retrieved October 19 from: http://floodrise.uci.edu/flood_hazard_viewer.
Fortunato, A.B., Oliveira, A., 2005. Influence of intertidal flats on tidal asymmetry. J. Coast. Res. 215, 1062–1067.
Friedrichs, C.T., Aubrey, D.G., 1988. Non-linear tidal distortion in shallow well-mixed estuaries: a synthesis. Estuar. Coast. Shelf Sci. 27, 521–545.
Fry, V., Aubrey, D.G., 1990. Tidal velocity asymmetries and bedload transport in shallow embayments. Estuar. Coast. Shelf Sci. 30, 453–473.
Gallien, T.W., Schubert, J.E., Sanders, B.F., 2011. Predicting tidal flooding of urbanized embayments: a modeling framework and data requirements. Coast. Eng. 58, 567–577.
Godin, G., 1985. Modification of river tides by the discharge. J. Waterw. Port Coast. Ocean. Eng. 111 (2), 257–274.
Godin, G., Martinez, A., 1994. Numerical experiments to investigate the effects of quadratic friction on the propagation of tides in a channel. Cont. Shelf Res. 14, 723–748.
Gong, W.P., Schuttelaars, H., Zhang, H., 2016. Tidal asymmetry in a funnel-shaped estuary with mixed semidiurnal tides. Ocean Dyn. 66, 637–658.
Groen, P., 1967. On the residual transport of suspended matter by an alternating tidal current. Neth. J. Sea Res. 3–4, 564–574.
Guo, L.C., van der Wegen, M., Roelvink, J.A., He, Q., 2014. The role of river discharge and tidal asymmetry on 1D estuarine morphodynamics. J. Geophys. Res. Earth Surf. 119. https://doi.org/10.1002/2014JF003110.
Guo, L.C., van der Wegen, M., Wang, Z.B., Roelvink, J.A., He, Q., 2016a. Exploring the impacts of multiple tidal constituents and varying river flow on long-term, large scale estuarine morphodynamics by means of a 1D model. J. Geophys. Res. Earth Surf. 120. https://doi.org/10.1002/2016JF003821.
Guo, W.Y., Song, D.H., Wang, X.H., Ding, P.X., Ge, J.Z., 2016b. Contributions of different tidal interactions to fortnightly variations in tidal duration asymmetry. J. Geophys. Res. Oceans 121, 5980–5994.

Hoitink, A.J.F., Hoekstra, P., van Maren, D.S., 2003. Flow asymmetry associated with astronomical tides: implications for the residual transport of sediment. J. Geophys. Res. 108 (C10), 3315–3322.
Holleman, R.C., Stacey, M.T., 2014. Coupling of sea level rise, tidal amplification, and inundation. J. Phys. Oceanogr. 44, 1439–1455.
Jewell, S.A., Walker, D.J., Fortunato, A.B., 2012. Tidal asymmetry in a coastal lagoon subject to a mixed tidal regime. Geomorphology 138, 171–180.
Kirwan, M.L., Murray, A.B., 2007. A coupled geomorphic and ecological model of tidal marsh evolution. Proc. Nat. Acad. Sci. 104 (15), 6112–6118.
Kopp, R.E., Horton, R.M., Little, C.M., Mitrovica, J.X., Oppenheimer, M., Rasmussen, D.J., Strauss, B.H., Tebaldi, C., 2014. Probabilistic 21st and 22nd century sea-level projection at a global network of tide-gauge sites. Earths Futur. 2, 383–406.
Lanzoni, S., Seminara, G., 2002. Long-term evolution and morphodynamic equilibrium to tidal channels. J. Geophys. Res. 107 (C1), 3001. https://doi.org/10.1029/2000JC000468.
Leonardi, N., Plater, A.J., 2017. Residual flow patterns and morphological changes along a macro- and meso-tidal coastline. Adv. Water Resour. 107, 290–301.
Lee, B.S., Li, M., Zhang, F., 2017. Impacts of sea level rise on tidal range in Chesapeake and Delaware Bays. J. Geophys. Res. Oceans 122, 3917–3938.
Lesser, G.R., Roelvink, J.A., van Kester, J.A.T.M., Stelling, G.S., 2004. Development and validation of a three-dimensional morphological model. Coast. Eng. 51, 883–915.
Lotze, H.K., Lenihan, H.S., Bourque, B.J., Bradbury, R.H., Cooke, R.G., Kay, M.C., Kidwell, S.M., Kirby, M.X., Peterson, C.H., Jackson, J.B.C., 2006. Depletion, degradation, and recovery potential of estuaries and coastal seas. Science 312, 1806–1809.
Nidzieko, N.J., 2010. Tidal asymmetry in estuaries with mixed semidiurnal/diurnal tides. J. Geophys. Res. 115, C08006. https://doi.org/10.1029/2009JC005864.
Postma, H., 1954. Hydrography of the Dutch Wadden Sea: A study of the relations between water movement, the transport of suspended materials, and the production of organic matter. Archives Néerlandaises de Zoologie 10 (4), 405–511.
Postma, H., 1961. Transport and accumulation of suspended matter in the Dutch Wadden Sea. Neth. J. Sea Res. 1, 148–190.
Ranasinghe, R., Pattiaratchi, C., 2000. Tidal inlet velocity asymmetry in diurnal regimes. Cont. Shelf Res. 20, 2347–2366.
Roos, P.C., Schuttelaars, H.M., 2015. Resonance properties of tidal channels with multiple retention basins: role of adjacent sea. Ocean Dyn. 65, 311–324.
Ruessink, B.G., van den Berg, T.J.J., van Rijn, L.C., 2009. Modeling sediment transport beneath skewed asymmetric wave above a plane bed. J. Geophys. Res. 114, C11021. https://doi.org/10.1029/2009JC005416.
Song, D.H., Wang, X.H., Kiss, A.E., Bao, X.W., 2011. The contribution of tidal asymmetry by different combinations of tidal constituents. J. Geophys. Res. 116, C12007. https://doi.org/10.1029/2011JC007270.
Speer, P.E., Aubrey, D.G., 1985. A study of non-linear tidal propagation in shallow inlet/estuarine systems. Part II: Theory. Estuar. Coast. Shelf Sci. 21, 207–224.
Stark, J., Smolders, S., Meire, P., Temmerman, S., 2017. Impact of intertidal area characteristics on estuarine tidal hydrodynamics: a modelling study for the Scheldt Estuary. Estuar. Coast. Shelf Sci. https://doi.org/10.1016/j.ecss.2017.09.004.
Stein, E.D., Cayce K., Salomon M., Bram D.L., De Mello D., Grossinger R., Dark S., 2014. Wetlands of the Southern California coasts- historical extent and change over time. SCCWRP Technical Report 826 (SFEI Report 720), pp. 1–58.
Thorne, K.M., MacDonald, G.M., Ambrose, R.F., Buffington, K.J., Freeman, C.M., Janousek, C.N., Brown, L.N., Holmquist, J.R., Gutenspergen, G.R., Powelson, K.W., Barnard, P.L., Takekawa, J.Y.. 2016. Effects of climate change on tidal marshes along a latitudinal gradient in California. U.S. Geological Survey Open-File Report 2016-1125, 75 pp, http://dx.doi.org/10.3133/ofr20161125.
Thorne, K., MacDonald, G., Guntenspergen, G., Ambrose, R., Buffington, K., Dugger, B., Freeman, C., Janousek, C., Brown, L., Rosencranz, J., Holmquist, J., 2018. US Pacific coastal wetland resilience and vulnerability to sea-level rise. Sci. Adv. 4 (2), eaao3270.
Trimble, S.W., 2003. Historical hydrographic and hydrologic changes in the San Diego creek watershed, Newport Bay. J. Hist. Geogr. 29, 422–444.
United Nations (UN, ed.), 2017. The First Global Integrated Marine Assessment: World Ocean Assessment I. Cambridge University Press, Cambridge. https://doi.org/10.1017/9781108186148.
van de Kreeke, J., Robaczewska, K., 1993. Tide-induced residual transport of coarse sediment: application to the Ems Estuary. Neth. J. Sea Res. 31 (3), 209–220.
van Rijn, L.C., 1993. Principles of Sediment Transport in rivers, Estuaries and Coastal Seas. Aqua Publications, the Netherlands.
Wang, Z.B., Jeuken, H., de Vriend, H.J., 1999. Tidal asymmetry and residual sediment transport in estuaries. WL Hydraulic, report No. Z2749, 66 pp.
Woodworth, P.L., Blackman, D.L., Pugh, D.T., Vassie, J.M., 2005. On the role of diurnal tides in contributing to asymmetries in tidal probability distribution function in areas of predominantly semi-diurnal tide. Estuar. Coast. Shelf Sci. 64 (2–3), 235–240.